Structural Engineering and Mechanics, *Vol. 69, No. 5 (2019) 579-589*
DOI: https://doi.org/10.12989/sem.2019.69.5.579

Behavioral trends of shear strengthened reinforced concrete beams with externally bonded fiber-reinforced polymer

Samer Barakat*, Salah Al-Toubat[a], Moussa Leblouba[b] and Eman Al Burai[c]

Department of Civil Engineering, University of Sharjah, Sharjah, P.O. BOX 27272, United Arab Emirates

(Received May 2, 2018, Revised January 23, 2019, Accepted January 24, 2019)

Abstract. Numerous experimental studies have been conducted on reinforced concrete (RC) beams strengthened in shear with externally bonded fiber reinforced polymer (EBFRP). The objectives of this work are to study the behavioral trends of shear strengthened EBFRP RC beams after updating the existing database. The previously published databases have been updated, enriched and cross checked for completeness, redundancy and consistency. The updated database now contains data on 698 EBFRP beams and covers the time span from 1992 to 2018. The collected database then refined applying certain filters and used to investigate and capture better interactions among various influencing parameters affecting the shear strength of EBFRP beams. These parameters include the type and properties of FRP, fiber orientation as well as the strengthening scheme, the shear and the longitudinal steel reinforcement ratios, the shear span ratio, and the geometry of the member. The refined database is used to test the prediction accuracy of the existing design models. Considerable scatters are found in the results of all tested prediction models and in many occasions the predictions are unsafe. To better understand the shear behavior of the EBFRP RC beams and then enhance the prediction models, it was concluded that focused experimental programs should be carried out.

Keywords: beam; fiber; FRP; reinforced concrete; shear strength

1. Introduction

In recent years, many studies have been conducted to understand the behavior of concrete structures strengthened with externally bonded fiber-reinforced polymer (EBFRP) and have resulted in valuable findings that incorporated into various national design guidelines such as ACI 440.2R-08, (2008), Canadian CSA-S806-02, (2002), European fib-TG9.3, Bulletin14, (2001) and CNR-DT 200/2004, (2004). Despite this large number of research studies for EBFRP members strengthened in shear, the experimental results obtained, and the theoretical models developed and used thus far are scarce and sometimes controversial.

The behavior of strengthened reinforced concrete members in shear is complicated and affected by several interacting parameters such as, type and properties of the FRP, fiber orientation as well as the strengthening scheme, the strength and composition of the concrete, the shear and the longitudinal steel reinforcement ratios, member geometry and size, the shear span ratio, the type of applied loading, in addition to the material behaviors of FRP, concrete, and steel.

Also, the complexity of the RC shear problem is increased by the addition of FRP composite strengthening materials that introduces a new set of variables related to the FRP composite, properties, behavior, systems and configurations. The aim of the research presented in this paper is to study the behavioral trends of shear strengthened EBFRP RC beams. To this end, three individual objectives are defined as follows: a) to update and filter the existing databases related to the shear strengthening of RC beams with EBFRP from the published literature, b) to bring together the most used existing models and investigate the different parameters that affect the shear strength of EBFRP RC beams and capture better interaction among various influencing parameters, c) To assess the prediction accuracy of the design models compared with the experimental results obtained from the filtered database.

2. Research significance

Since the last three decades, extensive experimental studies were performed on the EBFRP shear strengthening of reinforced concrete beams and several findings and conclusions were drawn as a result (e.g., Oller *et al*. 2019, Banjara and Ramanjaneyulu 2019, Duran *et al.* 2018, Al-Saikaly and Chaallal 2015). These studies have focused on exploring the effectiveness of EBFRP shear strengthening systems and configurations. But there is a large scatter between the theoretical models and the experimental results which indicates that other parameters that may influence the EBFRP shear resistance are not yet captured and many parameters interactions are still not fully discovered.

The complexity of shear behavior of RC beams is quite

* Corresponding author, Professor
E-mail: sbarakat@sharjah.ac.ae
[a]Professor
[b]Assistant Professor
[c]Engineer

ISSN: 1225-4568 (Print), 1598-6217 (Online)

high and is further increased in the presence of FRP strengthening systems. This paper attempts to identify and assess the most important factors that influence the shear failure of EBFRP strengthened RC beams by compiling and analyzing previously reported experimental data in the literature. These data are compiled in an updated database described herein.

3. Database of experimental data

Numerous experimental studies have been conducted on EBFRP RC beams strengthened in shear. The previously published databases presented by Gabriel (2011), Triantafillou (1998), Bousselham and Chaallal (2004, 2006, and 2008), Mofidi and Chaallal (2011), Chen *et al.* (2003, 2010, 2012), Kim *et al.* (2011, 2014, 2015), Li *et al.* (2018) among others, have been updated, enriched and cross checked for completeness, redundancy and consistency. The new database was subsequently updated and now contains data on 698 EBFRP RC beams and covers the time span from 1992 to 2018.

The upgraded database gathers all key variables that are known to have significant influence on the shear behavior of EBFRP RC beams such as: (i) the concrete strength, (ii) the shear and the tensile steel reinforcement ratios, (iii) the shear span to depth ratio (a/d), (iv) the cross section geometry and size, (v) the geometric, elastic and mechanical properties of the FRP and the strengthening configurations. In addition to this the mode of failure, load at failure V_{total}, and the contribution of the FRP to the shear resistance V_f are also reported. The upgraded database contains information on 698 experimental tests. The span length (L) of the tested beams is distributed as follows: 256 (37%) are with $(L < 2m)$, 325 (47%) are with $(2m < L < 4m)$, and 81 (12 %) are with $(L > 4m)$; no dimensions are specified for the remaining 36 beams (5%). The majority of the tested beams 524(75%) are of rectangular (R) cross-sections; the remaining 174 (25%) are of (T) cross-sections which are more widely used in practice.

The information on concrete compressive strength (f_c') of the tested EBFRP strengthened RC beams covers a wide range. 24% of beams has f_c' < 25 MPa, 68% has 25<f_c'<50, and 8% has f_c'>50 MPa. When needed the concrete tensile strength (f_{ct}) and modulus of elasticity (E_c) are obtained from the relevant specification in the ACI-08 (2007). About 75% of the data came from studies examining strong EBFRP RC beams with (f_c'>25MPa) to simulate the strengthening of relatively new structures. The rest of the data (25%) came from studies using relatively weak concrete to simulate the rehabilitation of old structures. The shear response of RC beam is closely related to the shear span to depth ratio (a/d). 30% of beams (208) are deep beams $(a/d \leq 2.5)$, 69% (482) are with $(a/d > 2.5)$; no (a/d) values are reported for the rest 1% (8) of beams. 52% of beams (363) are with shear reinforcement. 107 beams of those who have stirrups are deep beams $(a/d \leq 2.5)$ and 256 are regular beams. Of the 335 beams in the database that did not have shear reinforcement, 101 are deep beams and 234 regular beams. 96% of the beams have tensile reinforcement. As shown in Fig. 1, the types of fibers used for strengthening the EBFRP RC beams are Carbon FRP 85% (596), Glass FRP 11% (74) and Aramid FRP 4% (28). 320 of beams in the database are U wrapped, 207 Side (S) bonded, 135 W wrapped, 35 anchored U+ wrapped, and 1 anchored W+ wrapped (see Fig. 1). In 583 of beams in the database, the FRP is applied with 90° angle to longitudinal axis, 101 beams with 45°, and 14 beams with different angles. The tests of the database have limited experimental data on the behavior of pre-damaged RC beams strengthened in shear with the EBFRP. The database has information on data regarding beams that failed by diagonal shear cracking, beams that failed in flexure (FL) and beams for which no failure mode was reported (NA). Only, two modes of failure of the tested EBFRP beams related to the bond behavior at the concrete/FRP interface are considered. These modes are the debonding (DB) and rupture (RT) of the FRP composite at ultimate load. Of the beams in the database, DB failure occurred in 364 beams and RT failure in 201 beams, the rest failed in different modes. Fig. 2 presents the distributions of the collected database based on different criteria discussed above.

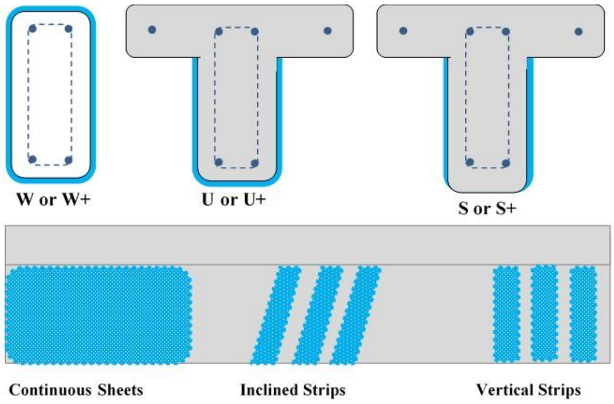

Fig. 1 Configurations used in shear strengthening of EBFRP RC beams

4. Refinement of the database

Since the focus of this work is to study the shear behavior of EBFRP RC beams, the database is refined by applying certain filters (adapted from Gabreil 2011) in order to have the most relevant information. Specifically:

1. Size of cross-section: Previous studies have showed that, to develop the bond resistance of the FRP composites, a minimum length of about $200mm$ is required. Therefore, data on beams with a height $h < 200mm$ are not included in the refined database;

2. Shear gain: Data on EBFRP strengthened beams that did not gain an increase in their shear capacities by more than 10% relative to the reference beams are also removed from the database. This is done to exclude the possibility that these beams have failed due to other unseen factors not related to the use of FRP;

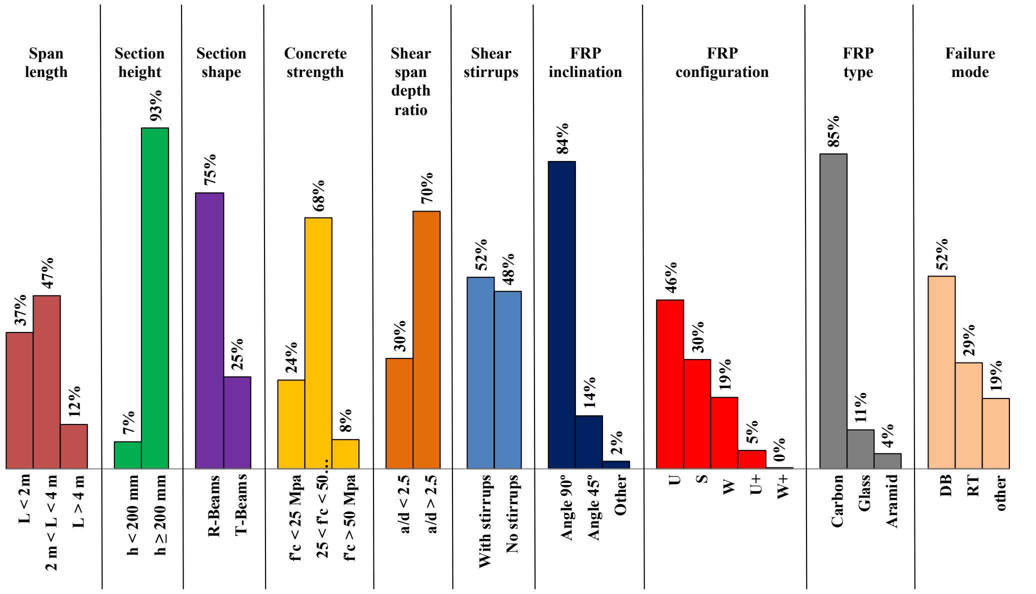

Fig. 2 Distributions of various parameters in the collected unrefined database

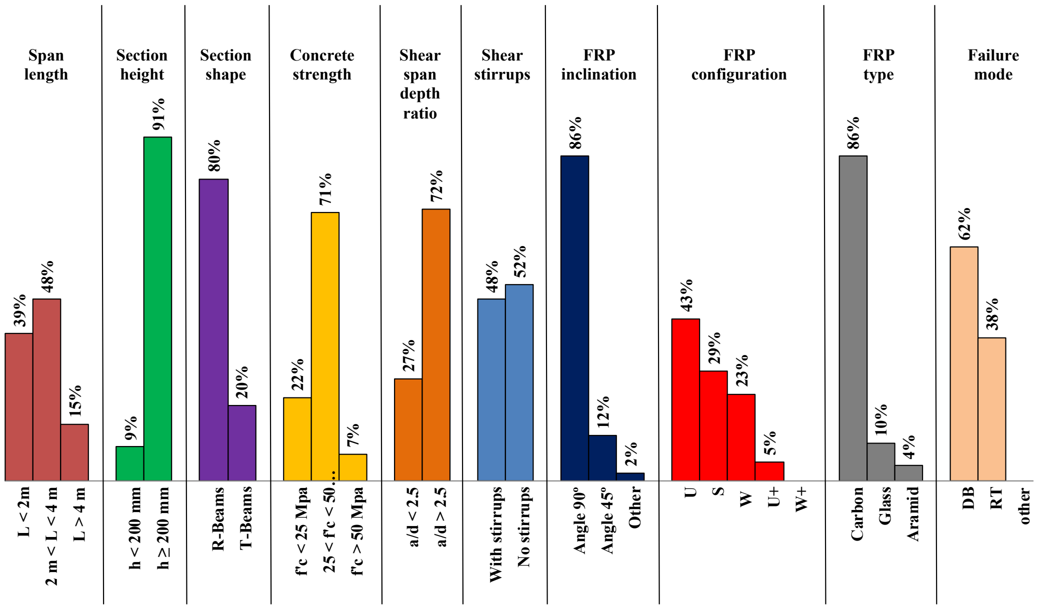

Fig. 3 ANN model output training data for upstream typhoon wind field coming from N direction with exponent 0.22

3. Failure mode: Data on beams that failed in mode different than diagonal shear cracking (debonding "DB" or rupture "RT") are disregarded.

After applying these filters, 49 beams that have height less than 200 mm were removed, 25 beams gaining shear force less than 10% and 152 beams having different mode of failures than debonding and rupture were also removed from the database. Data on 472 different beams remained for analysis in the refined database. Fig. 3 presents the distributions of the remaining database based on different criteria.

5. Analysis of the data

The effect of strengthening beams in shear with FRP is analyzed in this section in terms of the shear force gain taking into account the different failure modes for the beams. This gain equals the increase of the shear force due to the addition of FRP divided by the shear force of the control beam which is the beam before strengthening with FRP. The database will be analyzed in terms of the following parameters: a) the properties of the FRP composite; b) the influence of the FRP configuration (U-W-S-U+); c) the influence of the cross section (R-beams vs. T-beams); d) the shear span to depth ratio *a/d*; e) the beam size effect; f) the shear steel reinforcement ratio; and g) the longitudinal steel reinforcement ratio.

5.1 Analysis of the FRP properties

The influence of the properties of FRP is studied in

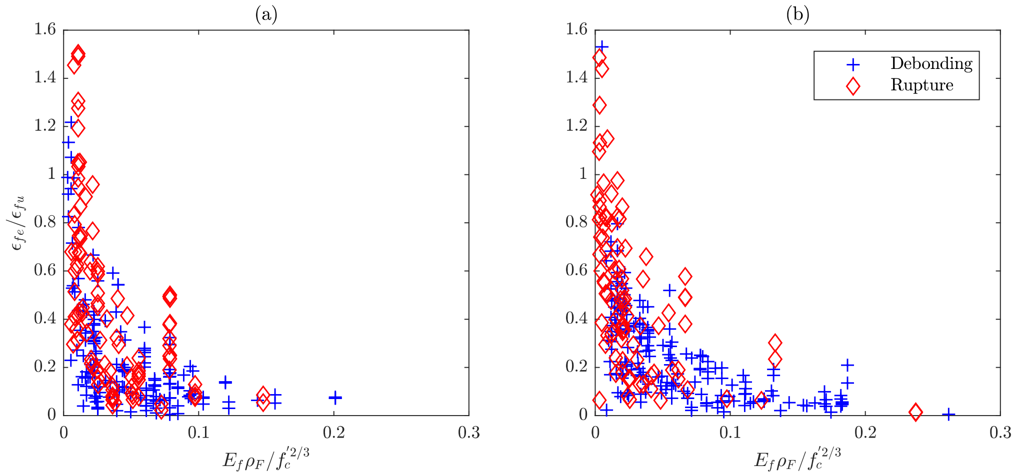

Fig. 4 Ratio of $\varepsilon_{fe}/\varepsilon_{fu}$ in terms of $E_f \rho_f / f_c^{\prime 2/3}$: (a) beams with stirrups; (b) beams without stirrups

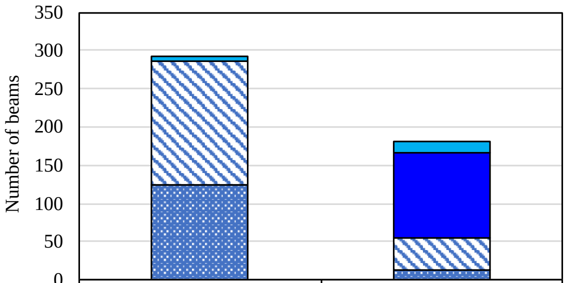

	Debonding (292-62%)	Rupture (180-38%)
U+	7	14
W	0	110
U	161	42
S	124	14

Fig. 5 Modes of failure in beams using different FRP configurations

terms of the ratio ε_{fe} to ε_{fu} where ε_{fe} and ε_{fu} are the FRP effective strain at failure and the ultimate strain given by the manufacturer respectively. As the FRP can't reach its full capacity, the effective strain ε_{fe} is limited to a fraction of the ultimate strain ε_{fu}. The contribution of FRP to the shear resistance can be expressed in terms of the FRP rigidity $E_f \rho_f$, the tensile strength of concrete, and the mode of failure. Fig. 4 shows the ratio of $\varepsilon_{fe}/\varepsilon_{fu}$ in terms of $E_f \rho_f / f_c^{\prime 2/3}$.

It is clear that the effective strain ε_{fe} decreases as the ratio $E_f \rho_f / f_c^{\prime 2/3}$ increases for both the beams having stirrups and the beams without stirrups for the two modes of failure, debonding and rupture. The values of $\varepsilon_{fe}/\varepsilon_{fu}$ seem to be higher for the rupture mode of failure.

5.2 The influence of FRP configuration

Fig. 5 shows that the side bonded and U-wrapped configurations are more likely to fail by debonding, while the W-wrapped and U+ -wrapped fail by rupture. It is interesting to note that 62% of the tested beams failed by debonding and only 38% by fiber rupture. The reason for debonding in the side bonded scheme is that the FRP is not anchored at the tension side of the beam, i.e., at the place of the flexural crack; and so it loses the adhesion and stops the developing of the effective strain. The presence of the shear stirrups in the beams will affect the effective strain in fibers depending on the FRP configuration.

Fig. 6 shows how the FRP strengthening systems influence the shear force gain in beams with and without stirrups. The efficiency of the strengthening configuration is different for beams with and without stirrups. As the $E_f \rho_f / f_c^{\prime 2/3}$ ratio increases, the shear force gains decrease for all strengthening configurations, but at low $E_f \rho_f / f_c^{\prime 2/3}$ ratios, the W-wrapped and U-wrapped beams performed better than S-bonded.

The increases in the shear force capacities are more when FRPs are used on beams without stirrups (Fig. 6(b)). However, for the same type of FRP configuration, the scatter of the shear force gains versus the values of $E_f \rho_f / f_c^{\prime 2/3}$ is quite large.

5.3 FRP configuration and utilization ratio $\varepsilon_{fe}/\varepsilon_{fu}$

As shown in Fig. 7, the effective strain ε_{fe} in FRP depends on the configuration S, U or W and also on the existence or nonexistence of stirrups. It can be noted that the ratio $\varepsilon_{fe}/\varepsilon_{fu}$ decreases as the ratio $E_f \rho_f / f_c^{\prime 2/3}$ increases for the two cases, the stirrups or no stirrups.

Looking at Figs. 7(a) and 7(c) where the beams failed by debonding, but one of them with stirrups and the other without; it can be observed that the strain utilization for the "U" scheme is higher or better than the "S" scheme; and for the beams that failed by rupture, Figs 7(b) and 7(d), the "W" schemes was better than the "U" scheme in providing the fiber utilization.

5.4 Influence of the cross-section R vs T-beams

The type of the beam cross section (R or T) can also affect the shear gain of the strengthened EBFRP beam. Fig. 8 shows the shear force gain in R and T-section beams with and without stirrups, for debonding and rupture failure

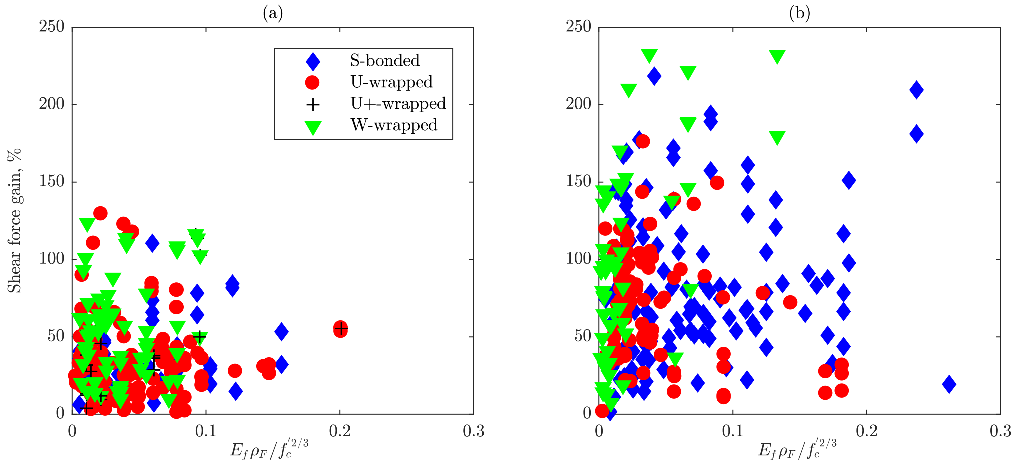

Fig. 6 Shear force grain versus $E_f \rho_f / f_c'^{2/3}$ ratio for different FRP configurations: (a) beams with stirrups; (b) beams without stirrups

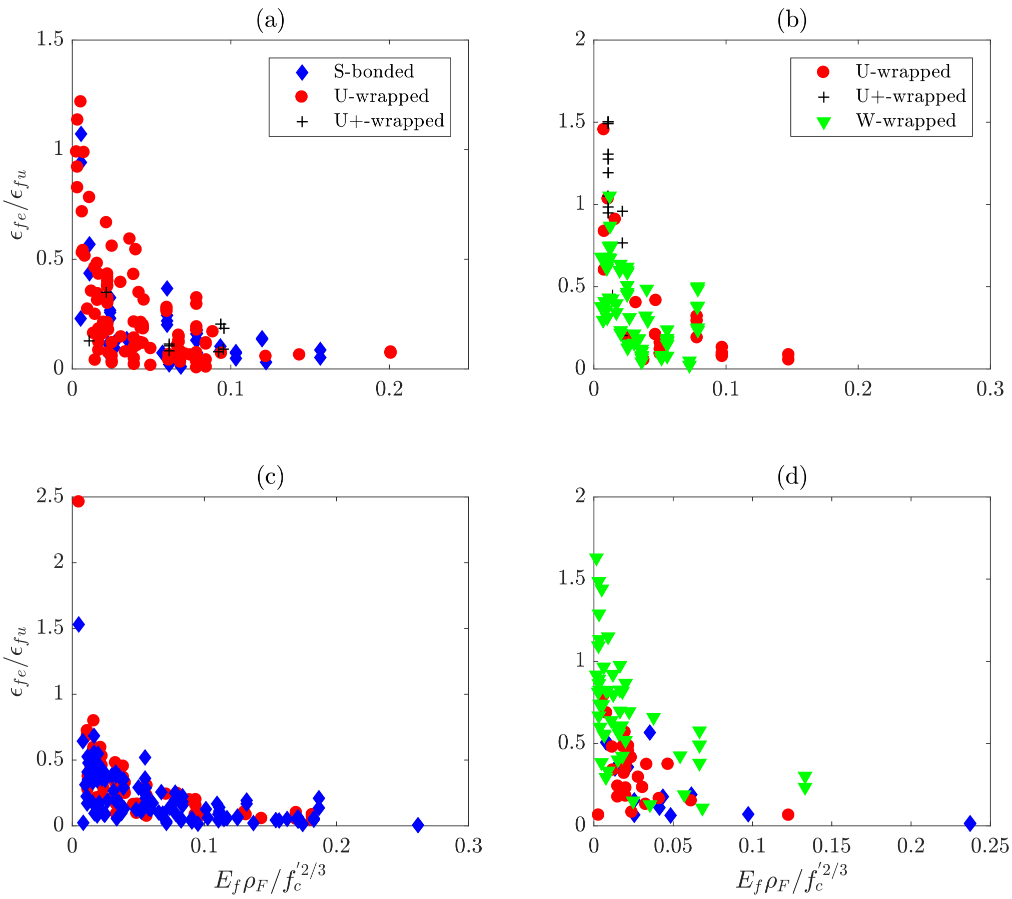

Fig. 7 Relation between the ratio $\varepsilon_{fe}/\varepsilon_{fu}$ and the strengthening scheme: (a) DB failure for beams with stirrups; (b) RT failure for beams with stirrups; (c) DB failure for beams without stirrups; (b) RT failure for beams without stirrups

mode of the FRPs. It is clear that the shear force gain in R-beams is much higher than that in T-beams for the two modes of failure. It is known that the T beams are practically more common than the R beams, but the theoretical models such as those derived from the regression analysis of the experimental data are adjusted using the R beams data, so the use of these models maybe unsafe.

5.5 Influence of the cross-section R vs T-beams

Fig. 9 presents the measured shear gain versus the shear span to depth ratio a/d. Beams with and without stirrups are considered separately. There are 247 of the beams in the database have stirrups, 62 of them have the ratio a/d less than or equal to 2.5 (i.e., deep beams) and 155 are regular beams while 8 beams are with unknown a/d ratio; on the other hand, there are 247 beams having no stirrups, 64 of them are deep beams and 183 are regular. It is clear from the graphs that the shear gain is higher in the regular beams

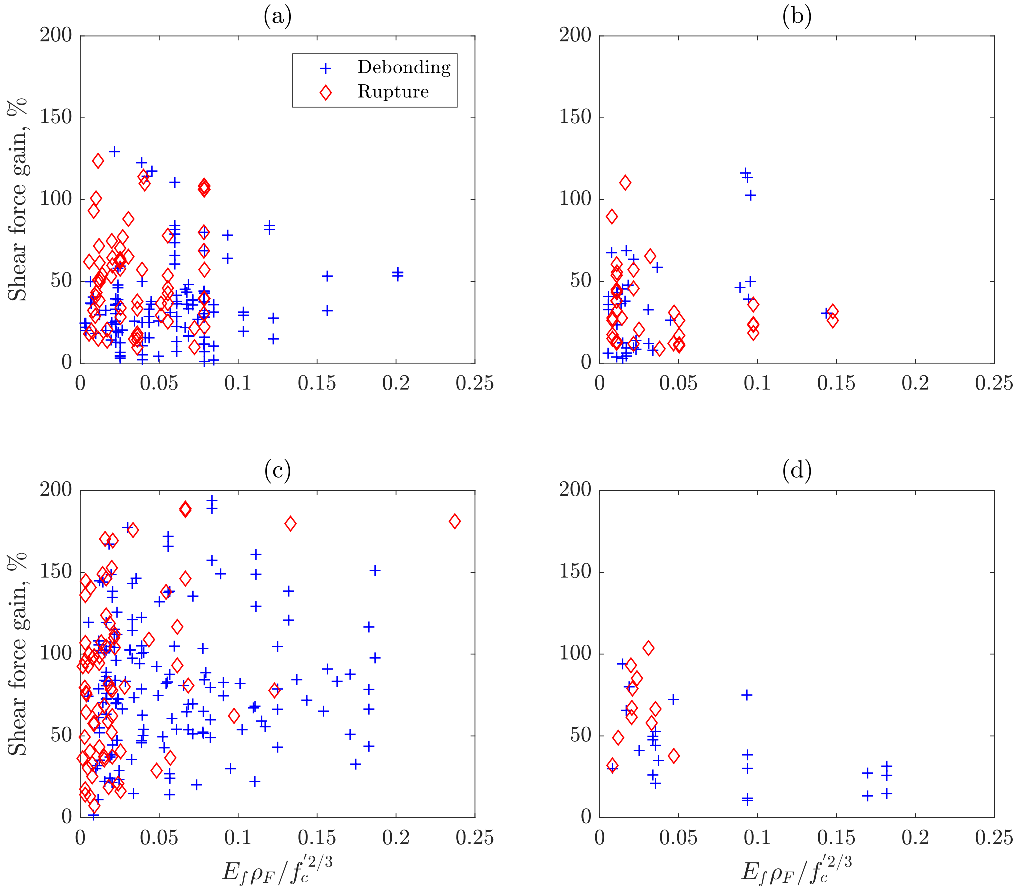

Fig. 8 Shear force gain versus $E_f\rho_f/f_c'^{2/3}$ in beams with and without stirrups for different cross section type: (a) R-beams with stirrups; (b) T-beams with stirrups; (c) R-beams without stirrups; (b) T-beams without stirrups

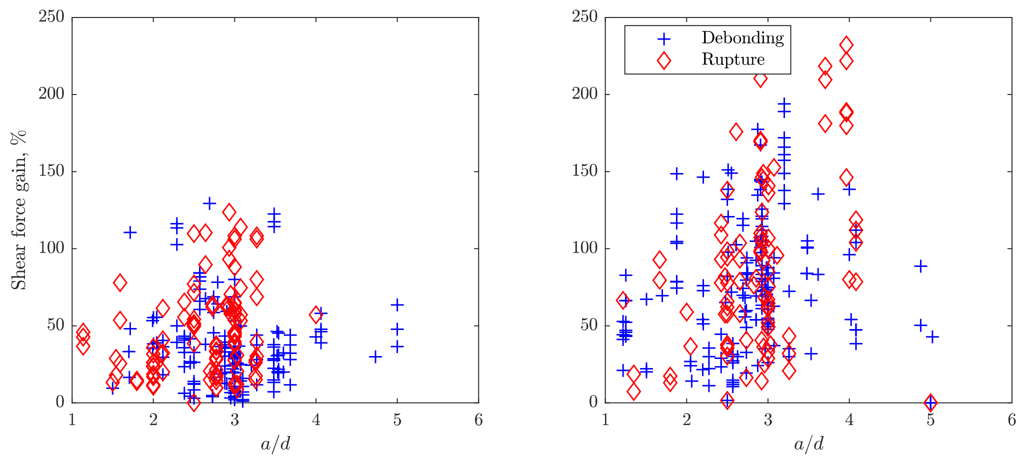

Fig. 9 Shear force grain versus shear span to depth ratio a/d: (a) beams with stirrups; (b) beams without stirrups

than the deep beams.

In general, for beams both with and without stirrups, the shear gain with the use of FRP increases with the a/d ratio until the latter reaches about 4.5; after this point, the gains are relatively small. It also seems that for deep beams $(a/d \leq 2.5)$ without and with stirrups, the predominant failure modes are debonding and rupture, respectively.

5.6 Effect of the beam's effective depth (scale effect)

The effect of the depth can also be studied; it was proven in many papers that the effect of the effective depth on the shear resistance appears in the beams without stirrups. Fig. 10 draws the relation between the effective depth and the shear force gain for different configurations and failures for beams without stirrups. Looking at Fig. 10, and specially at the beams failed by debonding, it is noticed that the shear gain is decreasing as the depth increases for values of effective depth less than 400 mm, the same note was reported by Challal (2011), but for d less than 300

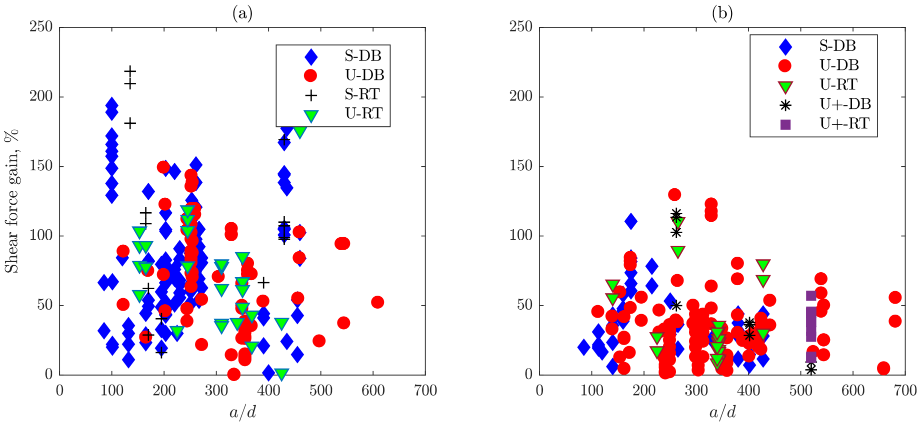

Fig. 10 Influence of the effective depth *d* on the shear force gain: (a) beams without stirrups; (b) beams with stirrups

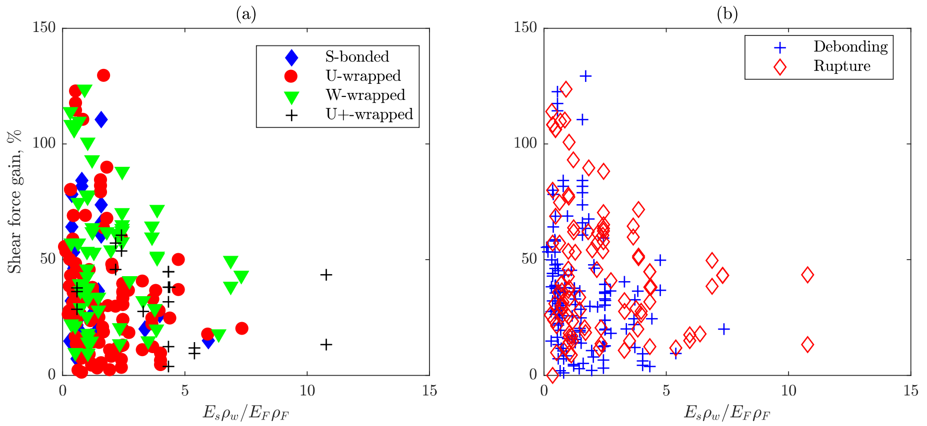

Fig. 11 Influence of the shear steel reinforcement on the shear force gain: (a) beams with stirrups; (b) beams without stirrups

mm. This note is opposite to what Triantafillou (1999) reported; he guessed that the shear force gain increases by increasing the bond surface area which means increasing the depth.

5.7 The transverse steel reinforcement

Fig. 11 shows the shear force gain relation with the ratio $E_s\rho_w/E_f\rho_f$. The graphs are detailed for the different strengthening schemes and for the two modes of failure debonding and rupture. It is clear that the transverse steel reinforcement strongly affects the shear gain in the beams.

The shear force gain decreases as the ratio $E_s\rho_w/E_f\rho_f$ increases; this means that the contribution of FRP will be week if the beam was reinforced heavily with stirrups, so the efficiency of FRP is always interacting with the stirrups and this interaction was reported in many studies by many authors (e.g., Li *et al.* 2018). Most of the papers that observed the interaction between the FRP and stirrups simply ignored it. They studied the effect of the variables in FRP with the presence of stirrups without decoupling their contributions, so this interaction is still not well understood.

5.8 The longitudinal steel reinforcement

Fig. 12 shows the plot of the ratio $E_s\rho_w/E_f\rho_f$ with the shear force gain. In Fig. 12(a), the shear force gain decreases as the ratio $E_s\rho_w/E_f\rho_f$ increases for the two modes of failure, debonding and rupture; and this means that the highest value of shear force gain that can be achieved by strengthening a beam having no stirrups with FRP is dependent on the amount of longitudinal steel reinforcement. Joint ACI-ASCE Committee 445 1998; CEN 1991 reported that the shear resistance of the concrete is related to the longitudinal steel reinforcement ratio and this would be the reason for the above observation.

6. RC beams shear design models

All of the design models rely on the approach where shear strength of a strengthened member, V_n is attained by the sum of the contributions from the concrete, V_c, reinforcing steel, V_s, and FRP, V_f as follows

$$V_n = V_c + V_s + V_f \tag{1}$$

Many studies revealed that the additive contribution models should be modified to account for the interaction among different parameters. For example, the shear steel reinforcement and applied FRP contributions to the total shear strength are additive but interacting. This interaction might depend on different factors.

6.1 ACI design models

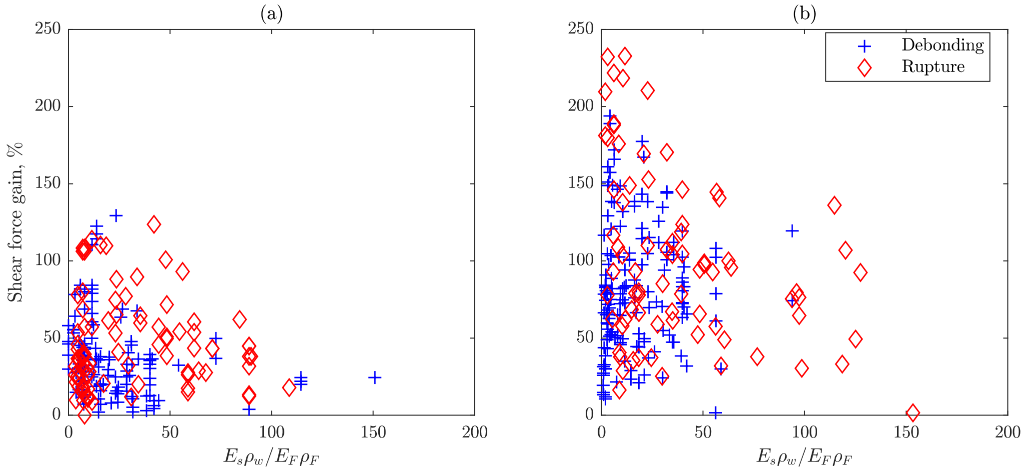

Fig. 12 Influence of longitudinal steel reinforcement on the shear force gain: (a) beams without stirrups; (b) beams with stirrups

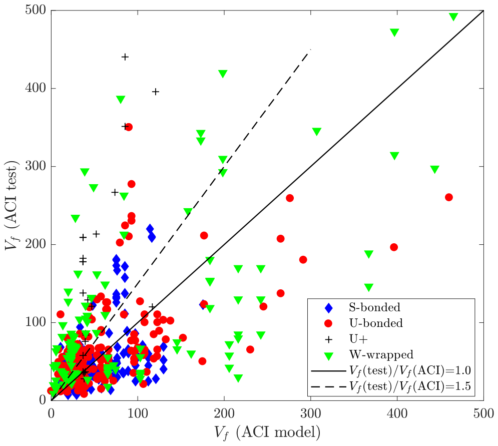

Fig. 13 Predictions of the ACI model for EBFRP RC beams based on FRP configuration

In ACI-318 (2007) and ACI 440 (2008), the total shear strength can be calculated as

$$V_c = 0.17\sqrt{f_c'}b_w d \tag{2}$$

$$V_s = \frac{A_{sw}f_y}{s}(\sin\alpha + \cos\alpha)d \tag{3}$$

$$V_f = \frac{A_{frp}f_{frp,e}(\sin\alpha + \cos\alpha)d_{frp}}{s_{frp}} \tag{4}$$

Where, f_c' is the specified concrete compressive strength, b_w and d are the width of the web and its effective depth, respectively. A_{sw} = area of the stirrups, f_y = yield stress of the stirrups, s = spacing of the stirrups and α = inclination of the stirrups.

$$A_{frp} = 2\,n\,t_{frp}\,w_{frp} \tag{5a}$$

$$f_{frp,e} = \varepsilon_{frp,e}\,E_{frp} \tag{5b}$$

$$\varepsilon_{frp,e} = \begin{cases} 0.004 \le 0.75\varepsilon_{frp,u} \text{ for full wrapping} \\ k_v\varepsilon_{frp,u} \text{ for side or U} - \text{jacketing} \end{cases} \tag{5c}$$

$$k_v = \frac{k_1k_2L_e}{11900\varepsilon_{frp,u}} \le 0.75\,;\; L_e = \frac{23300}{(n\,t_{frp}\,E_{frp,u})^{0.58}} \tag{5d}$$

$$k_1 = \left(\frac{f_c}{27}\right)^{\frac{2}{3}}$$
$$k_2 = \begin{cases} \dfrac{d_{frp} - 2L_e}{d_{frp}} \text{ for side bonding} \\ \dfrac{d_{frp} - L_e}{d_{frp}} \text{ for U} - \text{jacketing} \end{cases} \tag{5e}$$

6.2 FIB-14 (2001) shear design model

The FRP contribution to the shear strength is calculated as

$$V_{frp} = 0.9\rho_{frp}E_{frp}\varepsilon_{frp,ed}b_w d(\cot\theta + \cot\alpha)\sin\alpha \tag{6}$$

$$\varepsilon_{frp,ed} = \frac{\varepsilon_{frpk,e}}{\gamma_{frp}}\quad ;\quad \varepsilon_{frpk,e} = k\,\varepsilon_{frp,e} \tag{7}$$

$$\rho_{frp} = 2\frac{t_{frp}\sin\alpha}{b_w} \quad \text{for continuous sheets} \tag{8}$$

$$\rho_{frp} = 2\frac{t_{frp}w_{frp}}{b_w\,s_{frp}} \quad \text{for continuous sheets} \tag{9}$$

$$\varepsilon_{frp,e} = \begin{cases} \text{for W CFRP:} \\ 0.17\left(\dfrac{f_c^{\frac{2}{3}}}{E_{frp}\rho_{frp}}\right)^{0.3} \times \varepsilon_{frp,u} \\ \text{for U CFRP:} \\ \min\left[0.65\left(\dfrac{f_c^{\frac{2}{3}}}{E_{frp}\rho_{frp}}\right)^{0.56} \times 10^{-3}, \left(\dfrac{f_c^{\frac{2}{3}}}{E_{frp}\rho_{frp}}\right)^{0.3} \times \varepsilon_{frp,u}\right] \\ \text{For W AFRP:} \\ 0.48\left(\dfrac{f_c^{\frac{2}{3}}}{E_{frp}\rho_{frp}}\right)^{0.47} \times \varepsilon_{frp,u} \end{cases} \tag{10}$$

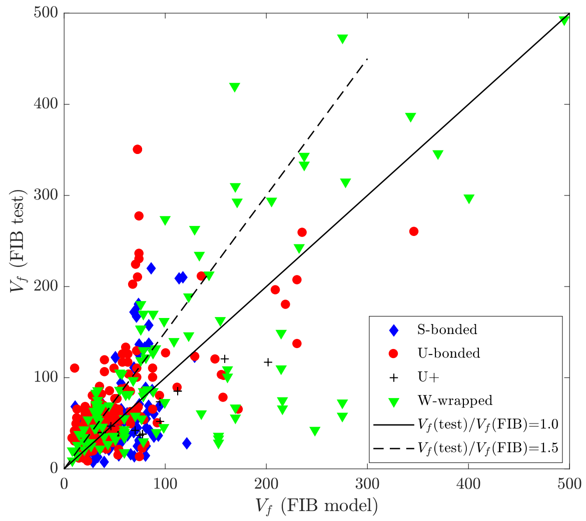

Fig. 14 Predictions of the FIB-14 model for EBFRP RC beams based on FRP configuration

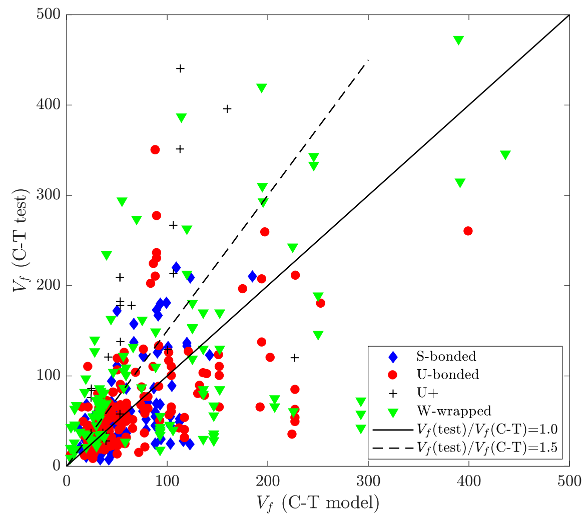

Fig. 15 Predictions of the Chen and Teng model for EBFRP RC beams based on FRP configuration

6.3 Chen & Teng's model (2003)

The FRP contribution to the shear strength is given by

$$V_{frp} = 2 f_{frp,e} w_{frp} t_{frp} \frac{h_{frp,e}(\cot\theta + \cot\beta)}{s_{frp}} \sin\beta \qquad (11)$$

$$h_{frp,e} = z_b - z_t \quad ; \quad z_t = d_{frp,t} \qquad (12)$$

$$f_{frp,e} = D_{frp(R,D)} \sigma_{frp,\max(R,D)} \qquad (13)$$

$$D_{frp,D} = \begin{cases} \dfrac{2}{\pi\,\lambda} \dfrac{1-\cos\left(\frac{\pi}{2}\lambda\right)}{\sin\left(\frac{\pi}{2}\lambda\right)\ \lambda} & \text{for } \lambda \le 1 \\ 1 - \dfrac{\pi - 2}{\pi\,\lambda} & \text{for } \lambda > 1 \end{cases} \qquad (14)$$

$$D_{frp,R} = \frac{1+\xi}{2} \quad ; \quad \xi = \frac{z_t}{z_b} \qquad (15)$$

$$\begin{aligned} z_b &= d_{frp,t}\left[d_{frp} - (h-d)\right] - 0.1d \\ &= 0.9d - (h - d_{frp}) \end{aligned} \qquad (16)$$

$$\sigma_{frp,\max(R,D)} = \min \begin{cases} f_{frp,u} \\ 0427\ \beta_w \beta_L \sqrt{\dfrac{E_{frp}\sqrt{f_c}}{t_{frp}}} \end{cases} \qquad (17)$$

$$\beta_L = \begin{cases} 1 & \text{for } \lambda \ge 1 \\ \sin\left(\dfrac{\pi\lambda}{2}\right) & \text{for } \lambda < 1 \end{cases} \quad ; \quad \lambda = \frac{L_{\max}}{L_e} \qquad (18)$$

$$\beta_L = \begin{cases} \dfrac{h_{frp,e}}{\sin\beta} & \text{for U} \\ \dfrac{h_{frp,e}}{2\sin\beta} & \text{for S} \end{cases} \quad ; \quad L_e = \sqrt{\frac{E_{frp} t_{frp}}{\sqrt{f_c}}} \qquad (19)$$

$$\beta_w = \sqrt{\frac{2 - \dfrac{w_{frp}}{s_{frp}\sin\beta}}{1 + \dfrac{w_{frp}}{s_{frp}\sin\beta}}} \quad ; \quad s_{frp} = \frac{w_{frp}}{\sin\beta} \qquad (20)$$

$$\sigma_{frp,\max,R} = f_{frp,u} \qquad (21)$$

7. Predictions of the design models

The predictions of the design models are compared with the experimental results obtained from the refined database (472 data tests). The comparisons between the predicted V_f by ACI, Fib-14, and Chen & Teng models (2010) and experimental FRP shear force (V_{test}) are shown respectively, in Figs. 13-15, for beams based on strengthening configuration and in Figs. 16-18, based on mode of failure. The design models exhibit the same trend in terms of the deviation of the predicted values from the experimental results. In general, the scatter of the predictions of the three design models is almost the same. It is clear that the predictions have large scatters around the equality lines. The predictions of the FRP shear contribution in several cases drastically underestimate (60%) or overestimate (40%) the capacity for EBFRP RC beams distributed as 35% for debonding mode of failure and 25% for rupture mode of failure (Fig. 10). Furthermore, Table 1 summarizes the ratio $V_{f(model)}/V_{f(Test)}$ statistics (μ = mean and σ = standard deviation). The three ratios experienced almost the same central tendency and dispersion. The Fib model shows relatively closer ratio values to 1.0 and smaller variations in terms of ($c.o.v$ = σ/μ = 0.83) compared to 0.85 and 0.86 for the ACI and Chen & Teng models. Many attempts were tried by the authors to enhance the predictions accuracy and reduce the scatter using multiple regression analysis but not yet successful to considerable levels. This may be attributed to many factors such as the sources of the gathered data are different and with different aims other than examining the effect of these variables on EBFRP behavior and the investigated parameters are varied simultaneously ignoring the coupling effect.

Table 1 Model prediction statistics

Configuration-failure mode-FRP type	Model Statistics					
	$V_{f(ACI)}/V_{f(Test)}$		$V_{f(Fib)}/V_{f(Test)}$		$V_{f(C\text{-}T)}/V_{f(Test)}$	
	μ	σ	μ	σ	μ	σ
S-DB-Ca	1.28	0.98	1.23	1.02	1.18	0.81
S-RT-Ca	0.89	0.65	1.12	1.04	2.14	1.82
S-DB-G	1.83	0.27	1.86	0.27	1.06	0.20
U-DB-Ar	1.39	0.49	1.28	0.44	1.45	0.55
U-RT-Ar	0.55	0.16	0.58	0.16	0.87	0.25
U-DB-Ca	1.02	0.79	0.91	0.70	1.06	0.62
U-RT-Ca	1.22	0.81	1.01	0.61	2.30	1.70
U-DB-G	1.49	0.98	1.07	0.65	1.45	0.74
U-RT-G	0.97	0.38	0.96	0.32	1.15	0.44
U+-DB-Ca	0.84	0.37	1.33	0.98	0.73	0.44
U+-RT-Ca	0.32	0.22	0.48	0.39	0.52	0.44
U+-DB-G	0.46		0.43		0.29	
W-RT-Ar	0.17	0.09	0.81	0.29	0.25	0.13
W-RT-Ca	1.29	1.20	1.28	1.23	1.50	1.38
W-RT-G	0.37	0.16	1.05	0.52	0.50	0.20
All Data	**1.10**	**0.93**	**1.08**	**0.89**	**1.22**	**1.05**

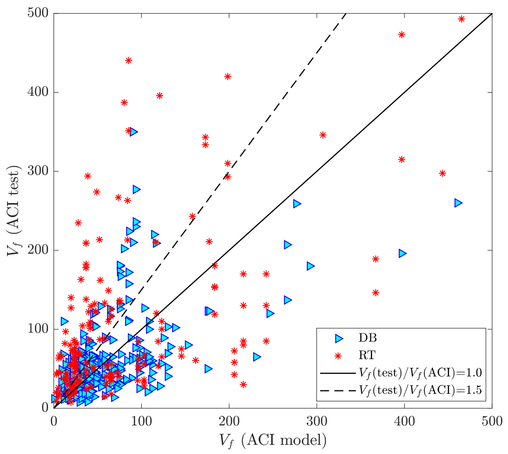

Fig. 16 Predictions of the ACI model for EBFRP RC beams based on FRP mode of failure

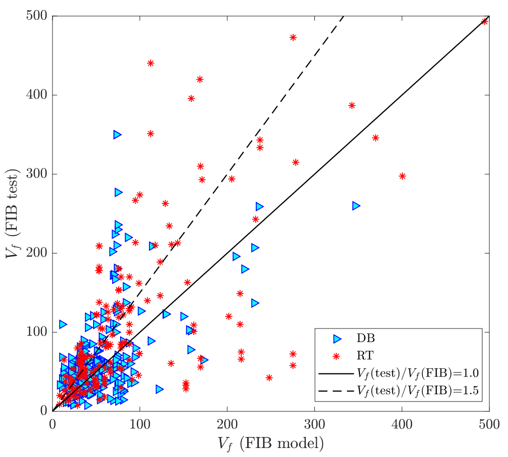

Fig. 17 Predictions of the FIB-14 model for EBFRP RC beams based on FRP mode of failure

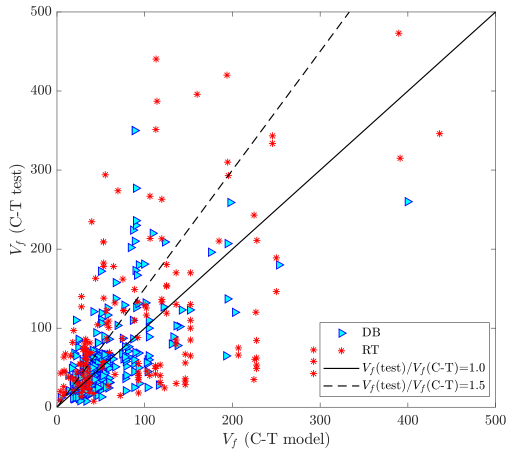

Fig. 18 Predictions of the Chen and Teng model for EBFRP RC beams based on FRP mode of failure

8. Conclusions

It is evident that a lot of research on the shear of EBFRP strengthened RC beams has been conducted and valuable data is available. Therefore, it is useful to compile all data in one database. This makes it easier to study and analyze the parameters that most influence the shear behavior of RC members strengthened with EBFRP. The initially compiled data base contained 698 tests, but in many cases, the data obtained from such tests are unreliable, and incomplete that led to a refined database with 472 tests. The analysis of this available data confirmed that the shear problem involves a number of parameters, which are related and interacting such as the properties of FRP and the existence of the internal shear reinforcement among others. It must be noted that the data was gathered from different experimental tests. It follows that the data analysis and the interpretation of the results should be handled with great caution. The ongoing investigations by the authors are aiming at reducing the scatter in the prediction of the design models presented above by analyzing the refined database. The authors believe that to get a full understanding and rational explanations of the relationships among variables affecting the behavior of EBFRP in shear requires sufficient and focused experimental programs. Then the results of such programs can be used to develop/calibrate applicable design models, which will accurately simulate the shear behavior of EBFRP RC members.

Acknowledgements

This work was supported by the Sustainable Construction Materials and Structural Systems (SCMASS) research group, University of Sharjah (grant #18020401100-P). This support is highly acknowledged.

References

ACI 318 (2007), *Building Code Requirements for Structural*

Concrete and Commentary, American Concrete Institute, Farmington Hills, Michigan, U.S.A.

Al-Rousan, R.Z. (2017), "Shear behavior of RC beams externally strengthened and anchored with CFRP composites", *Struct. Eng. Mech.*, **63**(4), 447-456.

Banjara, N.K. and Ramanjaneyulu, K. (2019), "Effective CFRP retrofit strategy for flexural deficient RC beams", *Struct. Eng. Mech.*, **69**(2), 163-175.

Banthia, N., Bisby, L., Britton, R., Cheng, R., Falli, G. and Hutchinson, R. (2004), *An Introduction to FRP Strengthening of Concrete Structures Composites for Construction*, ISIS Canada.

Belarbi, A., Bae, S.W. and Brancaccio, A. (2012), "Behavior of full-scale RC T-beams strengthened in shear with externally bonded FRP sheets", *Constr. Build. Mater.*, **32**, 27-40.

Bousselham, A. and Chaallal, O. (2004), "Shear strengthening reinforced concrete beams with fiber-reinforced polymer: Assessment of influencing parameters and required research", *ACI Struct. J.*, **101**(2), 219-227.

Bousselham, A. and Chaallal, O. (2006), "Behavior of reinforced concrete T-beams strengthened in shear with carbon fiber-reinforced polymer-an experimental study", *ACI Struct. J.*, **103**(3), 339-348.

Bousselham, A. and Chaallal, O. (2008), "Mechanisms of shear resistance of concrete beams strengthened in shear with externally bonded FRP", *J. Compos. Constr.*, **12**, 449-512.

Chen, G.M. Teng, J.G. and Chen, J.F. (2010), "RC beams shear strengthened with FRP: Shear resistance contributed by FRP", *Mag. Concrete Res.*, **62**, 301-311.

Chen, G.M., Teng, J.G. and Chen, J.F. (2012), "Shear strength model for FRP-strengthened RC beams with adverse FRP-steel interaction", *J. Compos. Constr.*, **17**(1), 50-66.

Chen, G.M., Teng, J.G., Chen, J.F. and Rosenboom, O.A. (2010), "Interaction between steel stirrups and shear-strengthening FRP strips in RC beams", *J. Compos. Constr.*, **14**(5), 498-510.

Chen, J.F. and Teng, J.G. (2003), "Shear capacity of fiber-reinforced polymer-strengthened reinforced concrete beams: Fiber reinforced polymer rupture", *J. Struct. Eng.*, **129**(5), 615-625.

Chen, J.F. and Teng, J.G. (2003), "Shear capacity of FRP-strengthened RC beams: FRP debonding", *Constr. Build. Mater.*, **17**(1), 27-41.

CNR-DT-200 (2014), *Guide for the Design and Construction of Externally Bonded FRP Systems for Strengthening Existing Structures*.

Committee ACI 440.2R (2008), *Guide for the Design and Construction of Externally Bonded FRP Systems*, American Concrete Institute.

Deniaud, C. and Cheng, J. (2004), "Simplified shear design method for concrete beams strengthened with fiber reinforced polymer sheets", *J. Compos. Constr.*, **8**(5), 425-433.

Dias, S.J.E. and Barros, J.A.O. (2010), "Performance of reinforced concrete T beams strengthened in shear with NSM CFRP laminates", *Eng. Struct.*, **32**(2), 373-384.

Duran, B., Tunaboyu, O., Kaplan, O. and Avsar, O. (2018), "Effectiveness of seismic repairing stages with CFRPs on the seismic performance of damaged RC frames", **67**(3), 233-244.

El-Saikaly, G. and Chaallal, O. (2015), "Fatigue behavior of RC T-beams strengthened in shear with EB CFRP L-shaped laminates", *Compos. Part B: Eng.*, **68**, 100-112.

Fib 14 TG 9.3 (2001), *Externally Bonded FRP Reinforcement for RC Structures*.

Grande, E., Imbimbo, M. and Rasulo, A. (2009), "Effect of transverse steel on the response of RC beams strengthened in shear by FRP: Experimental study", *J. Compos. Constr.*, **13**(5), 405-414.

Khan, U., Al-Osta, M.A. and Ibrahim, A. (2017), "Modeling shear behavior of reinforced concrete beams strengthened with externally bonded CFRP sheets", *Struct. Eng. Mech.*, **61**(1), 125-142.

Kim, Y. (2011), "Shear behavior of reinforced concrete T-beams strengthened with carbon fiber reinforced polymer sheets and CFRP anchors".

Kim, Y., Quinn, K., Ghannoum, W.M. and Jirsa, J.O. (2014), "Strengthening of reinforced concrete T-beams using anchored CFRP materials", *ACI Struct. J.*, **111**, 1027-1036.

Kim. Y., Ghannoum, W.M. and Jirsa, J.O. (2015), "Shear behavior of full-scale reinforced concrete T-beams strengthened with CFRP strips and anchors", *J. Constr. Build. Mater.*, **94**, 1-9.

Li, W., Hu, C., Pan, Z., Peng, W., Yang, Y. and Xing, F. (2018) "A proposed strengthening model considering interaction of concrete-stirrup-FRP system for RC beams shear-strengthened with EB-FRP sheets", *J. Reinf. Plast. Compos.*, **37**(10), 685-700.

Liang, J.F., Yu, D., Xie, S. and Li, J. (2017), "Flexural behaviour of reinforced concrete beams strengthened with NSM CFRP prestressed prisms", *Struct. Eng. Mech.*, **62**(3), 2428-2444.

Mofidi, A. and Chaallal, O. (2011), "Shear strengthening of RC beams with EB FRP: Influencing factors and conceptual debonding model", *J. Compos. Constr.*, **15**(1), 62-74.

Oller, E., Pujol, M. and Marí, A. (2019), "Contribution of externally bonded FRP shear reinforcement to the shear strength of RC beams", *Compos. Part B: Eng.*, **164**, 235-248.

Pellegrino, C. and Modena, C. (2002), "Fiber reinforced polymer shear strengthening of reinforced concrete beams with transverse steel reinforcement", *J. Compos. Constr.*, **6**(2), 104-111.

Pellegrino, C. and Modena, C. (2006), Fiber-reinforced polymer shear strengthening of reinforced concrete beams: Experimental study and analytical modeling", *ACI Struct. J.*, **103**(5), 720-728.

Sas, G. (2011), "FRP shear strengthening of reinforced concrete beams", Ph.D. Dissertation, Lulea University of Technology, Lulea, Sweden.

Sas, G., Taljsten, B., Barros, J., Lima, J. and Carolin, A. (2009), "Are available models reliable for predicting the FRP contribution to the shear resistance of RC beams?", *J. Compos. Constr.*, **13**(6), 514-534.

Triantafillou, T.C. (1998), "Shear strengthening of reinforced concrete beams using epoxy-bonded FRP composites", *ACI Struct. J.*, **95,** 107-115.

Triantafillou, T.C. and Antonopoulos, C.P. (2000), "Design of concrete flexural members strengthened in shear with FRP", *J. Compos. Constr.*, **4**(4), 198-205.

Vincenzo, C. (2013), "Shear interaction effect between transverse reinforcements in FRP-strengthened RC beams", *Compos. Part B Eng.*, **45**(1), 1222-1233.

Zhou, C., Ren, D. and Cheng, X. (2017), "Shear-strengthening of RC continuous T-beams with spliced CFRP U-strips around bars against flange top", *Struct. Eng. Mech.*, **64**(1), 135-143.

CC